S-Parameter Characterization and Modeling of Three-Terminal Semiconductive Devices at Cryogenic Temperatures

J. W. Smuk, *Member, IEEE*, M. G. Stubbs, *Member, IEEE*, and J. S. Wight, *Senior Member, IEEE*

***Abstract*—Three generations of three-terminal microwave semiconductive devices are measured and analyzed at 297K and 77K. FET's, HEMT's, and Pseudomorphic-HEMT's (P-HEMT's) are accurately characterized over the frequency range from 1 GHz to 20 GHz using a newly developed split-block test fixture and the Through-Reflect-Line (TRL) calibration technique. Accurate characterization allows small-signal models to be closely fitted at both temperatures. The performance improvement offered by low temperature operation is described.**

I. Introduction

BY applying an extremely accurate microwave characterization technique, the behavior of three generations of three-terminal microwave semiconductive devices are observed over a large change in temperature. Measured *S*-parameters are used to derive equivalent small-signal models of FET, HEMT and P-HEMT devices. Analysis of the changes in the intrinsic model elements with temperature allows the suitability of the three devices for use at cryogenic temperatures to be determined.

The results and technique should be useful in the realization of cryogenic semiconductive circuitry such as is presently applied to the fields of radioastronomy and satellite communications [1]. In addition, development of hybrid semiconductive/superconductive microwave integrated circuitry operating at liquid nitrogen temperatures, using semiconductive active devices coupled with superconductive passive structures, should benefit from this work [2].

II. Measurement Apparatus And Technique

The apparatus consists of a customized cold head on an RMC Cryosystems LTS-22-IR helium refrigerator coupled with a Hewlett Packard 8510B automatic vector network analyzer. Semi-rigid coaxial cables connect the split-block test fixture, mounted on the cold head, to coaxial feedthroughs which in turn are connected to the network analyzer test ports. The test fixture halves provide the through and reflect calibration standards as well as the input/output lines to connect the device under test. An earlier paper describes the apparatus, TRL calibration method and test fixture construction in more detail [3]. The three-terminal semiconductive device die are epoxy attached onto 508-μm wide shims that are sandwiched between the test fixture halves, as shown in Fig. 1. Thermocompression bonded gold wires connect the die to the input/output lines.

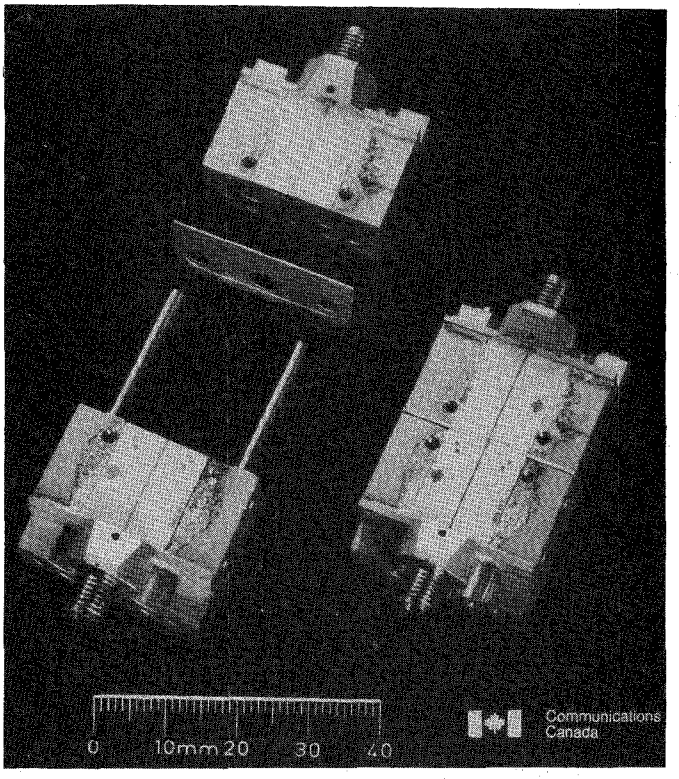

Fig. 1. Split-block test fixture with LNF001 P-HEMT: disassembled and assembled.

III. Results And Interpretation

Measured and modeled *S*-parameters of a 0.25 μm $\times$ 100 μm Fujitsu FHR10X HEMT at both 300 K and 77 K are shown from 1 GHz to 20 GHz in Fig. 2. The effects of the input/output bond wires on these results have not been removed to demonstrate the extent of de-embedding offered by this technique. The measurements are relatively resonance free, allowing subtle changes in all *S*-parameters to be observed. Major changes with temperature reduction are confined to increased transmission gain and decreased output

Manuscript received October 21, 1991.

J. W. Smuk and M. G. Stubbs are with the Communications Research Centre, 3701 Carling Avenue, P.O. Box 11490, Station H, Ottawa, ON, K2H 8S2, Canada .

J. S. Wight is with the Department of Electronics, Carleton University, Ottawa, ON, K1S 5B6, Canada .

0162–8828/92$03.00 © 1992 IEEE

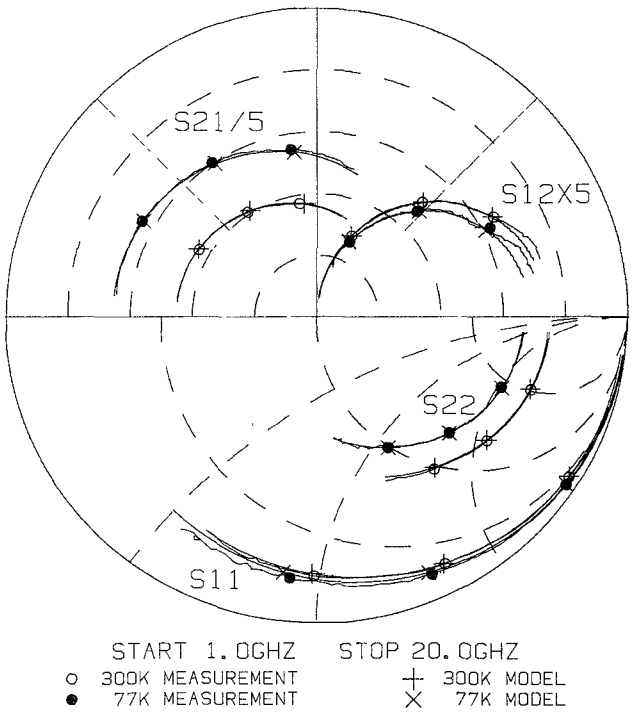

Fig. 2. Measured and modeled S-parameters of a FHR10X HEMT (markers at 5, 10, and 15 GHz).

TABLE I
BIAS CONDITIONS

	NE673		FHR10X		LNF001	
	297 K	77 K	297 K	77 K	297 K	77 K
V_D (V)	3.0	3.0	2.0	2.0	2 .0	2 .0
I_{DSS} (mA)	34	26	26	26	18*	11*
I_{DS} (mA)	13	10	5	5	6	6

* Enhancemant device: values at $V_{gs} = +0.5$ V.

impedance. The rougher traces at 77 K are due to the drift of the network analyzer during the lengthened calibration and measurement cycle. Similar responses for a 0.3 μm × 280 μm NEC NE673 FET and a 0.25 μm × 150 μm Comsat LNF001 P-HEMT [4] were also obtained. A doubling in $|S_{12}|$ of the P-HEMT when cooled was the only significant deviation. Operating conditions for the devices, biased for minimum noise figure, are shown in Table I.

The three-terminal device model of Fig. 3 was fitted to the measured S-parameters using FETlink software [5]. The model incorporates the standard FET model with additional parasitics. Although originally developed for FET's, Fig. 2 illustrates how closely this physics based program fits the FHR10X. Similar fits for the NE673 and LNF001 were also obtained. The model elements for the three devices at both temperatures as well as the calculated cutoff frequencies are shown in Table II. FETlink requires an Rg value, which in this case is obtained through an initial Supercompact optimization; all other values result from the fit. Negative values for Rd, Rs, and Lg result from the nonphysical basis of the equivalent circuit model [6]. Input/output inductance values for the same device differ at the

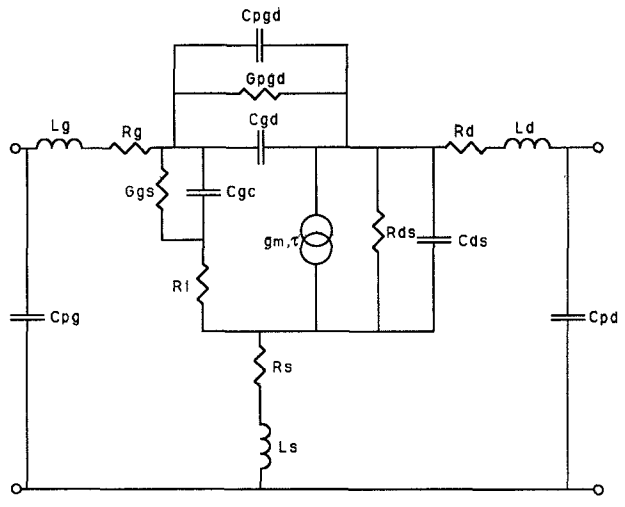

Fig. 3. FETlink small-signal model.

two temperatures since different bond wires connect the die into the test fixture following calibrations at each temperature. In the case of the LNF001, the device was wafer probed at room temperature.

At 77 K, the NE673 exhibits a large increase in transconductance, a small drop in transit time and the largest decrease in output resistance, resulting in a cutoff frequency increase of 35%. The FHR10X shows the largest percentage increase in transconductance, the largest percentage decrease in transit time and a smaller drop in output resistance, resulting in a 54% higher cutoff frequency. This follows from the increased carrier mobility at lower temperatures due to fewer phonon collisions in the lightly doped layer which confines the 2-D gas in a HEMT. The zero value of Ri at 77 K is not possible and shows the software or measurement accuracy may need to be improved if small gate periphery devices are to be correctly analyzed at cryogenic temperatures. The LNF001 exhibits a large increase in transconductance, a large decrease in transit time and the smallest drop in output resistance. Again, this is due to the enhanced mobility of the 2-D gas in the P-HEMT structure. However, a substantial increase in Cgc results in a 13% drop in cutoff frequency. An increase in Cds at 77 K is also observed and both effects are believed due to deep levels decreasing depletion zone widths.

IV. SUMMARY

Techniques that accurately measure and closely fit equivalent small-signal models to three-terminal semiconductive devices at cryogenic temperatures have been demonstrated. Of the three devices characterized, the FHR10X exhibits the largest improvement in performance at cryogenic temperatures due to its mobility enhancement and defect free structure. These results and technique will be useful in the field of cryogenic microwave electronics, where small-signal equivalent models are useful for both gain and noise matching.

REFERENCES

[1] T. Saito, Y. Ohashi, and H. Kurihara, "A Cryogenic 28-GHz-band low-noise amplifier for radio astronomy," in *3rd Asia–Pacific Microwave*

TABLE II
LINEAR MODEL ELEMENT VALUES

	NE673		FHR10X		LNF001	
	297 K	77 K	297 K	77 K	297 K	77 K
gm (mS)	50.9	72.8	26.9	42.5	37.5	55.7
Cgc (pF)	0.309	0.317	0.116	0.113	0.185	0.322
Ggs (mS)	0.137	0.213	0	0.077	0.037	0.134
Rds (Ω)	230	124	334	232	461	371
Ri (Ω)	3.7	1.9	2.2	0	7.5	1.5
τ (ps)	3.5	2.9	1.9	0.8	4.2	2.1
Cgd (pF)	0.024	0.035	0.015	0.021	0.011	0.011
Cds (pF)	0.100	0.093	0.058	0.063	0.035	0.070
Lg (nH)	0.119	0.125	0.135	0.161	0.007	0.161
Rg (Ω)	2.0	2.0	1.0	0.5	2.0	1.0
Ld (nH)	0.104	0.202	0.089	0.148	0.100	0.100
Rd (Ω)	-0.24	-2.1	2.8	5.6	-11.9	1.5
Ls (nH)	0.021	0.017	0.021	0.024	-0.002	0.009
Rs (Ω)	1.0	1.8	0.8	1.0	-1.8	0.75
Cpg (pf)	0.01	0.01	0.02	0.02	0	0
Cpd (pf)	0	0	0	0	0	0
Cpgd (ff)	15	2	6	0	14	5
Gpgd (mS)	0	0	0.007	0	0.039	0
f_T (GHz)	24.3	32.9	32.7	50.5	30.4	26.6

Conf. Proc., 1990, pp. 661–664.
[2] T. Van Duzer and S. Kumar, "Semiconductor-superconductor hybrid electronics," in *Low Temp. Electron. Conf.*, Apr. 23–26, 1990.
[3] J. W. Smuk, M. G. Stubbs, and J. S. Wight, "An enhanced microwave characterization technique for cryogenic temperatures," *Electron. Lett.*, vol. 26, pp. 2127–2129, 1990.
[4] G. Metze *et al.*, "Monolithic V-band pseudomorphic-MODFET low-noise amplifiers," *IEEE MTT Symp. Dig.*, 1989, pp. 199–204.
[5] Copyright GaAsCode Ltd, Cambridge, England.
[6] P. H. Ladbrooke, A. J. Hill, and J. P. Bridge, "Negative *Rs* and *Rd* in GaAs FET and HEMT equivalent circuits," *Electron. Lett.*, vol. 26, pp. 680–681, 1990.